

Important pickup coupling effect on ${}^8\text{He}(p,p)$ elastic scattering

F. Skaza^a, N. Keeley^a, V. Lapoux^{a,1,2}, N. Alamanos^a,
F. Auger^a, D. Beaumel^b, E. Becheva^b, Y. Blumenfeld^b,
F. Delaunay^b, A. Drouart^a, A. Gillibert^a, L. Giot^c,
K.W. Kemper^d, R.S. Mackintosh^e, L. Nalpas^a, A. Pakou^f,
E.C. Pollacco^a, R. Raabe^{a,3}, P. Roussel-Chomaz^c,
J.-A. Scarpaci^b, J-L. Sida^{a,4}, S. Stepantsov^g, R. Wolski^{g,h}

^a*CEA-Saclay, DSM/DAPNIA/SPhN, F-91191 Gif-sur-Yvette, France*

^b*Institut de Physique Nucléaire, IN2P3-CNRS, F-91406 Orsay, France*

^c*GANIL, Bld. Henri Becquerel, BP 5027, F-14021 Caen Cedex, France*

^d*Department of Physics, Florida State University, Tallahassee, Florida
32306-4350, USA*

^e*Department of Physics and Astronomy, The Open University, Milton Keynes,
MK7 6AA, UK*

^f*Department of Physics, University of Ioannina, 45110 Ioannina, Greece*

^g*Flerov Laboratory of Nuclear Reactions, JINR, Dubna, RU-141980 Russia*

^h*The Henryk Niewodniczański Institute of Nuclear Physics, PL-31342 Kraków,
Poland*

Abstract

The ${}^8\text{He}(p,p)$ and (p,d) reactions were measured in inverse kinematics at 15.7 A·MeV and analyzed within the coupled reaction channels framework, the (p,d) cross section being particularly large. We find that coupling to ${}^8\text{He}(p,d)$ pickup has a profound effect on the ${}^8\text{He}(p,p)$ elastic scattering, and that these strong coupling effects should be included in analyses of proton elastic and inelastic scattering. Through its modification of the elastic scattering wave functions this coupling will strongly affect the extraction of spectroscopic information such as the relationship between neutron and proton nuclear deformations, with important consequences for our understanding of the structure of exotic nuclei.

Key words: ${}^8\text{He}(p,p)$, (p,d) , coupled reaction channels calculations, dynamic polarization potential

PACS: 25.60.Bx, 25.60.Je, 24.10.Eq

Strong coupling effects in low-energy nuclear reactions are well established for heavy-ion collisions, and lead to important modifications of the effective nucleus-nucleus interaction. The $^{16}\text{O} + ^{208}\text{Pb}$ system is a well documented example, with coupled reaction channels (CRC) calculations showing how inelastic scattering and transfer channels generate a dynamic polarization potential (DPP) with a substantial real part [1,2], having important consequences for elastic scattering and fusion.

Important effects on (p,p) elastic scattering due to coupling to (p,d) pickup have been demonstrated for stable nuclei [3–5]. The effect is particularly large for light nuclei [4], reducing with increasing target mass and incident proton energy, although remaining significant for 50 MeV protons incident on ^{64}Zn . Pickup coupling was also found to significantly affect inelastic scattering, mainly through the modification of the elastic scattering wave functions [3], leading to significant changes in the extracted deformation parameters. However, the possibility of such strong coupling effects has come to be ignored in analyses of proton elastic and inelastic scattering, although a recent study of $^6\text{He}(p,p)$ postulated the existence of a repulsive real DPP due to breakup that gave improved agreement with the data [6], subsequently further investigated through coupled discretized continuum channels (CDCC) calculations [7].

We report here a measurement of $^8\text{He}(p,p)$ scattering at 15.7 A·MeV incident energy. Data for $^8\text{He}(p,d)$ populating the $3/2^-$ ground state resonance of the unbound ^7He measured in the same experiment have been previously reported [8], and the cross section is found to be very large. This should therefore be a case where (p,d) coupling will have an important influence on the $^8\text{He}(p,p)$ scattering. We present CRC calculations including $^8\text{He}(p,d)$ pickup to the $3/2^-$ ground state of ^7He which demonstrate the profound influence of this coupling on the elastic scattering and, hence, on the nucleon-nucleus interaction in a way that falls outside the scope of local-density folding models.

The ^8He beam was produced by the ISOL technique and accelerated to 15.7A·MeV by the CIME cyclotron at the SPIRAL facility [9], with no contaminants. The maximum (average) intensity in the experiment was 14000 (5000) p/s. The proton target was a 8.25 mg/cm² thick polypropylene (CH_2)_n foil. The detection system consisted of the MUST array [10] to detect the light charged particles, a plastic wall for the detection of the projectile-like fragment, and two beam tracking detectors (CATS) upstream of the target. The position sensitive CATS detectors [11] were used to improve the definition of the beam position and incident angle on target. They provided particle by particle po-

¹ Corresponding author

² E-mail: vlapoux@cea.fr

³ Present address: IKS, University of Leuven, B-3001 Leuven, Belgium

⁴ Present address: CEA DIF/DPTA/SPN, B.P. 12, F-91680 Bruyères-le-Châtel, France

sition and time tracking of the beam.

The MUST array consists of eight three-stage telescopes, each $6 \times 6 \text{ cm}^2$. The first stage is a $300 \mu\text{m}$ -thick double-sided Si-strip detector which provides horizontal and vertical position, time-of-flight (TOF) with respect to the beam detectors, and energy loss of the recoil proton. The second stage is a 3 mm-thick Si(Li) giving the energy for protons up to 25.4 MeV, and the third stage a 1.5 cm-thick CsI allowing the detection of protons up to 75 MeV in energy. The array was assembled in a wall configuration located 15 cm from the target. The wall was placed in two positions, covering the angular range between 30° – 90° (lab.). At this distance, the 1 mm wide strips result in an angular resolution of 0.4° (lab.) for the detection of the scattered particle.

For the less energetic recoil particles stopped in the first stage, e.g. protons with energies below 6 MeV, mass identification was obtained using the energy versus TOF technique. Particles were identified in the correlation plot of their energy loss, ΔE , in the Si-strip detector versus their TOF. The TOF was measured between the Si-stage and the start signal given by the passage of the incident particle through the second CATS detector. Protons from 6 to 25 MeV were unambiguously identified by the ΔE -E method using energy loss measurements in the Si Strip and the Si(Li) detectors. The energy resolution obtained varied between 600 keV and 1 MeV, depending on target thickness and the reaction kinematics. Events with a p or d in coincidence with the heavy ejectile, plus a particle detected in the two CATS detectors to provide the incident beam trajectory, were retained to build the kinematical spectra and subsequently extract the (p,p) and (p,d) angular distributions.

The elastic data extend from 20° – 110° , and the transfer data from 27° – 85° , in their respective center of mass (c.m.) systems. To measure angular distributions from 40° down to 20° (c.m.) where the energy of the recoiling protons decreases to 1.5 MeV, a 1.48 mg/cm^2 polypropylene target was used. To obtain good statistics at large angles, from 40° to 110° (c.m.), a 8.25 mg/cm^2 target was used. The overall values for the statistical plus systematic errors in the angular distributions arise from the detection efficiency and reconstruction process, which gives $\pm 5 \%$ uncertainty, including the effect of background subtraction ($\pm 2 \%$); the target thickness ($\pm 5\%$); and the efficiency in the detection of the incident particles ($\pm 2\%$). This results in a total uncertainty of $\simeq \pm 7.5 \%$ in the normalization of the data for elastic scattering and transfer to the ${}^7\text{He}$ ground state.

In Fig. 1 the measured elastic scattering angular distribution is compared to optical model calculations performed within the framework of the microscopic nucleon-nucleus JLM potential [12], using a no-core shell model ${}^8\text{He}$ density [13]. The JLM potential is complex and the data for well-bound nuclei were found to be well reproduced with slight variations of the real and

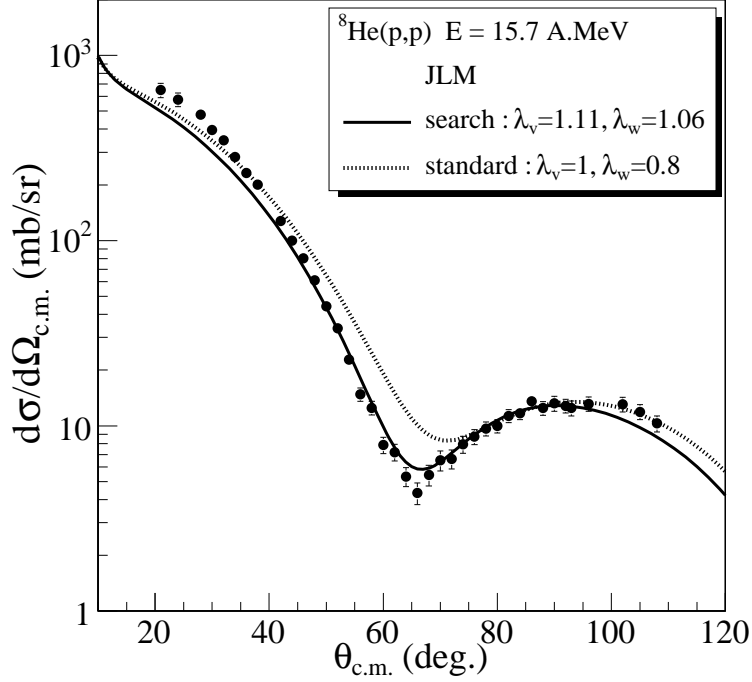


Fig. 1. Optical model calculations using the JLM potential compared to the ${}^8\text{He}+p$ elastic scattering data. See text for details.

imaginary parts, V and W . The required normalization factors, λ_V and λ_W , respectively, are found to be close to unity. For well-bound light nuclei ($A \leq 20$), the only modification required is $\lambda_W = 0.8$ [14], adopted as a “standard” normalization.

The standard JLM (dotted curve) does not reproduce the data. Best agreement was obtained with $\lambda_V = 1.11$, $\lambda_W = 1.06$ (solid curve), but the data at angles smaller than 40° (c.m.) are significantly underpredicted. It should be emphasized that simply modeling the DPP by a renormalization of the JLM potential is unable to reproduce the whole angular range of the data.

Clearly, we need to include explicitly in our calculations the effect of coupling to other reaction channels. To investigate the effect of coupling to (p,d) pickup on ${}^8\text{He}(p,p)$ scattering a series of CRC calculations was carried out using the code FRESKO [15]. The JLM prescription was retained for the $p+{}^8\text{He}$ optical potential. We should include in the coupling scheme, *a priori*, the following reactions: elastic, inelastic scattering and transfer reactions to the ground or excited states of the nuclei produced in the exit channel, either in bound or resonant states. But this requires the corresponding inputs, transition strengths to the excited states and spectroscopic factors. To simplify, we limitate the coupling scheme to the main channels which may contribute significantly in terms of angular distributions in the domain treated in our analysis. The experimental observations can help us in determining which states should be included

in the coupling scheme, or not. In the ${}^8\text{He}(p,p')$ experiment at 72 A·MeV reported in Ref. [16], the first excited state of ${}^8\text{He}$ was found to be a 2^+ located at 3.6 MeV. The cross sections measured between 20° to 50° (c.m.) were found to lie below 1 mb/sr; a weak excitation of the 2^+ ${}^8\text{He}$ was found [17]. In our experiment, as mentioned in Ref. [8], inelastic (p,p') to the 2^+ excited state was also selected. These cross sections at 15.7 A·MeV will be presented and analyzed in a forthcoming article. Compared to the angular distributions of the (p,d) transfer reaction, they were found to be twice up to 5 times lower in the angular range from 20° to 80° (c.m.). We also face the problem of the exit channel of the (p,d) reaction. It is beyond the scope of present CDCC calculations to include within the coupling scheme the continuum of the unbound ${}^7\text{He}$ states and calculate the transfer reaction. The best calculation which can be performed, at the present stage, is to consider the deuteron states within the continuum. In Ref. [18], Halderson showed that the recoil corrected continuum shell model predictions support a low-lying $1/2^-$ excited state for ${}^7\text{He}$ at 1 MeV, as found by Meister et al. [19]. Our recent results [8] also indicated this low-lying excited state of ${}^7\text{He}$; it is weakly excited, and roughly the cross sections are 10 times lower than the $(p,d){}^7\text{He}_{gs}$ ones. In Ref. [20], at 50A·MeV, a resonance at 2.9 MeV was observed in ${}^7\text{He}$, the cross sections (from 5° to 15° (c.m.)) were found to be 5 times less than the $(p,d){}^7\text{He}_{gs}$. Consequently, in our analysis, we did not explicitly include the coupling to the ${}^7\text{He}$ excited states and we considered (p,p) and $(p,d){}^7\text{He}_{gs}$ as the main coupled reactions.

The CDCC formalism was employed in the exit channel, as described in Ref. [21]. The bare $d+{}^7\text{He}$ potential was of Watanabe type [22], the n and p plus ${}^7\text{He}$ optical potentials being calculated using the global parametrization of Koning and Delaroche [23]. Couplings to deuteron breakup with the neutron and proton in relative S and D states were explicitly included using the CDCC formalism and the coupling scheme presented in Fig. 2.

For the transfer step, the neutron-proton overlap was calculated using the Reid soft-core potential [24], including the D -state component of the deuteron ground state. The same interaction was used to calculate the exit channel deuteron potentials. The $n+{}^7\text{He}$ binding potential was a Woods-Saxon well with the “standard” geometry of $R_0 = 1.25 \times A^{1/3}$ fm, $a = 0.65$ fm, the well depth being adjusted to give the correct binding energy. The spin-orbit term was omitted as it has no effect on the calculated cross section. Transfers to unbound states of the “deuteron” were included in addition to that to the deuteron ground state. The full complex remnant term and non-orthogonality correction were also included.

There were three adjustable parameters, the real and imaginary normalizations of the JLM entrance channel potential and the spectroscopic factor for the ${}^8\text{He}(0^+)/{}^7\text{He}(3/2^-)$ overlap. All three were adjusted to obtain the optimum simultaneous agreement with the elastic scattering and transfer data.

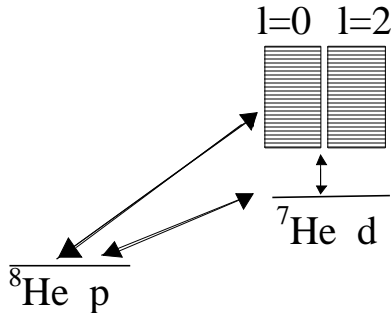


Fig. 2. Coupling scheme used in the CRC calculations.

The normalization of the (real) JLM spin-orbit potential was constrained to be the same as that of the real central potential.

In Fig. 3 we present the calculated angular distributions for ${}^8\text{He}(p,p)$ and ${}^8\text{He}(p,d)$ compared to the data. The results shown are for the final calculation with JLM normalization factors $\lambda_V = 1.05$, $\lambda_W = 0.2$. A ${}^8\text{He}(0^+)/{}^7\text{He}(3/2^-)$ spectroscopic factor of $C^2S = 3.3$ gave the best agreement with the data, slightly smaller than the value (4.1 ± 1.3) obtained in the CCBA analysis of ref. [8], but within the quoted uncertainty.

Excellent agreement between the calculated and measured elastic scattering is obtained over the whole angular range, which was not possible in the optical model calculations shown in Fig. 1. The very large effect of the (p,d) coupling on the elastic scattering is evident. Note that in the full CRC calculation the pickup coupling generates a considerable fraction of the total absorption; only a small component of the JLM imaginary potential is retained ($\lambda_W = 0.2$), which may be mostly attributed to compound nucleus effects. For comparison, the no-coupling calculation using the bare JLM potential with $\lambda_V = 1.05$, $\lambda_W = 0.2$ is also shown in Fig. 3.

The agreement between the calculated and measured (p,d) angular distributions is less good, the calculations overpredicting the data for angles greater than 50° in the c.m. system. This is probably due to the use of global potentials as a basis for the exit channel bare potential and could be improved by tuning the potential parameters, although we have chosen not to do so to show the quality of agreement that may be obtained with such potentials.

The large change in the elastic scattering induced by the pickup coupling may be represented as a substantial DPP. To obtain the local and L -independent representation of this DPP, we followed the procedure which was used to obtain the DPP for the ${}^6\text{He}+p$ system in Ref. [7]. The elastic scattering S -matrix is generated by the full CRC calculations (including coupling processes), and the total local optical potential is obtained by subjecting this S -matrix to an inversion procedure $S_{ij} \rightarrow V(r)$. The inversion is carried out using the

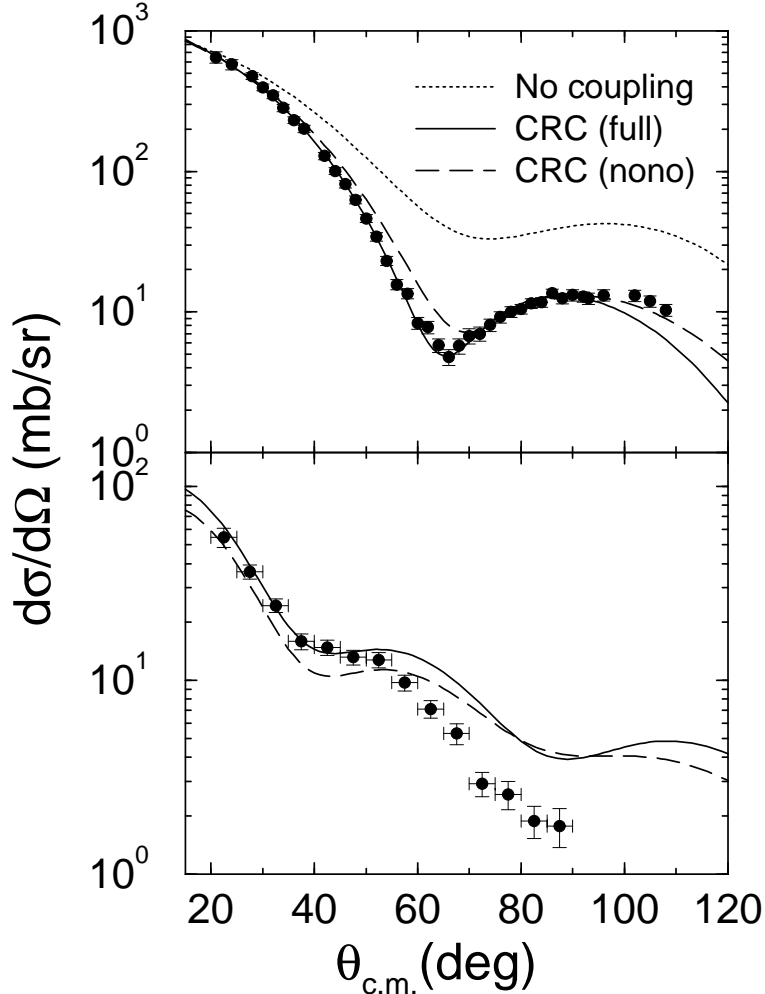


Fig. 3. ${}^8\text{He}(p,p)$ (upper panel) and ${}^8\text{He}(p,d)$ (lower panel) calculations compared to the data. The solid curves denote the full CRC calculation with $\lambda_V = 1.05$, $\lambda_W = 0.2$ and the dotted curve indicates the no-coupling calculation with the same bare potential. The dashed curves denote the result of a CRC calculation omitting the non-orthogonality correction.

iterative-perturbative inversion method of Kukulin and Mackintosh [25] which can give very reliable potentials, including spin-orbit potentials for the spin-half case, for all relevant radii. The bare diagonal proton potential (i.e without coupling) of the CRC calculation is then subtracted from $V(r)$ and the remainder is identified as the DPP. The result is shown in Fig. 4 for two cases, the solid line being the DPP in the case of the full CRC calculation and the dashed line the DPP from the CRC calculation with the non-orthogonality correction omitted. Previous calculations [3–5,26] omitted the latter, but the qualitative finding that pickup leads to substantial repulsion as well as absorption is confirmed. We find that the non-orthogonality correction changes the shape of the real DPP in particular, so that for a ${}^8\text{He}$ target it is largely in the nuclear center. For this reason, the effect on the real central volume integral, as

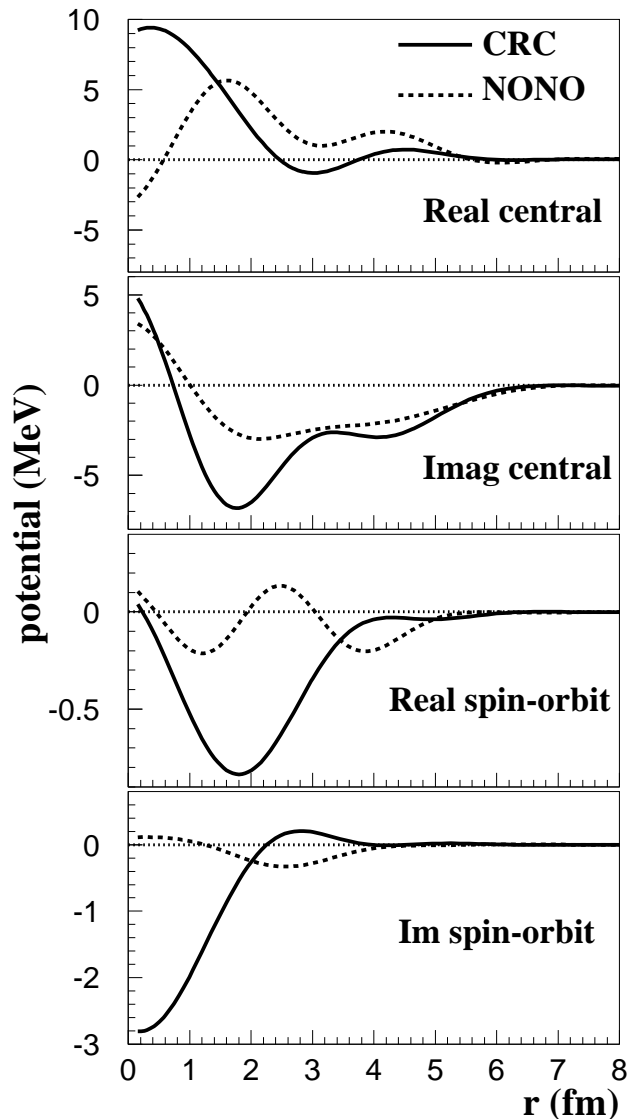


Fig. 4. DPP generated by the ${}^8\text{He}(p,d)$ coupling obtained as explained in the text. presented in Table 1, is just 7%.

Other features of the DPP are a significant imaginary spin-orbit term and an emissive imaginary central term at the nuclear center. Emissivity at the nuclear center often occurs in local representations of a fundamentally non-local and, in principle, L -dependent potential [25]. This emissivity and the other characteristics of the radial form of the DPP (accounting for the better fit to elastic scattering than renormalized JLM potentials), can be traced to the fact that the contribution of the pickup coupling to the effective nucleon-nucleus potential lies outside the scope of what could be described within the framework of folding models based on an underlying local-density approximation. We therefore conclude that the inclusion of pickup coupling is essential for a

	J_R	$\langle r^2 \rangle_R^{1/2}$	J_I	$\langle r^2 \rangle_I^{1/2}$	J_{SOR}	J_{SOI}
OM	704.14	3.092	55.37	3.336	26.60	0.005
CRC	653.94	2.938	307.47	4.138	40.27	1.25
NONO	571.28	2.840	252.62	4.360	33.15	6.55

Table 1

Volume integrals per nucleon pair/(MeV fm³), and rms radii/fm of the bare potential (OM) and the potentials found by inversion for the full CRC calculation and for the CRC calculation in which the non-orthogonality term was omitted (NONO).

complete understanding of proton scattering.

The modification of the elastic scattering wave functions by the pickup coupling also has important implications for proton inelastic scattering and the information that may be drawn therefrom. If one follows the usual conventions and renormalizes the transition potentials by the same factors as the entrance channel optical potential, be they of phenomenological form or calculated microscopically from theoretical transition densities, the effect on the level of agreement with data will be important. A full investigation of the magnitude of this effect for the L=2 ⁸He(p,p') transition to the 2⁺ first excited state is left for a later comprehensive article, but test calculations using collective model form-factors show a decrease of 14 % in the nuclear deformation length extracted from a CRC calculation compared to that obtained from a DWBA calculation.

To summarize, we have shown that for a particular case, ⁸He, the explicit inclusion of (p,d) coupling has a profound influence on the calculated elastic scattering. Combined with the results of previous studies for stable nuclei [3–5,26], we may infer that this effect is probably general throughout the chart of the nuclides. Evidently, an investigation of the systematics of the effect to determine under what circumstances it is most pronounced would be of great interest. However, it appears necessary to measure the (p,d) reaction and include this effect in analyses of proton scattering for radioactive beams if correct inferences are to be drawn. Through its modification of the elastic scattering wave function the pickup coupling will also have an important influence on the calculated inelastic proton scattering, with all that this implies for the extraction of information such as M_n/M_p ratios from data for this process.

References

- [1] I.J. Thompson et al., Nucl. Phys. A 505 (1989) 84.
- [2] S.G. Cooper and R.S. Mackintosh, Nucl. Phys. A 513 (1990) 373.

- [3] R.S. Mackintosh, Nucl. Phys. A 209 (1973) 91.
- [4] R.S. Mackintosh, Nucl. Phys. A 230 (1974) 195.
- [5] R.S. Mackintosh, A.A. Ioannides, and I.J. Thompson, Phys. Lett. B 178 (1986) 1.
- [6] V. Lapoux et al., Phys. Lett. B 517 (2001) 18.
- [7] R.S. Mackintosh and K. Rusek, Phys. Rev. C 67 (2003) 034607.
- [8] F. Skaza et al., submitted to Phys. Rev. C.
- [9] A.C. Villari et al., Nucl. Phys. A 693 (2001) 465.
- [10] Y. Blumenfeld et al., Nucl. Instrum. Methods A 421 (1999) 471.
- [11] S. Ottini et al., Nucl. Instrum. Methods A 431 (1999) 476.
- [12] J.-P. Jeukenne, A. Lejeune, and C. Mahaux, Phys. Rev. C 16 (1977) 80.
- [13] P. Navrátil and B.R. Barrett, Phys. Rev. C 57 (1998) 3119.
- [14] J.S. Petler et al., Phys. Rev. C 32 (1985) 673.
- [15] I.J. Thompson, Comput. Phys. Rep. 7 (1988) 167.
- [16] A.A. Korshennikov et al., Phys. Lett. B **316** (1993) 38.
- [17] L.V. Chulkov, C.A. Bertulani et A.A. Korshennikov, Nucl. Phys. A**587** (1995) 291.
- [18] D. Halderson, Phys. Rev. C **70**, 041603 (2004).
- [19] M. Meister et al., Phys. Rev. Lett. **88**, 102501 (2002).
- [20] A.A. Korshennikov *et al.*, Phys. Rev. Lett. **82**, 3581 (1999).
- [21] N. Keeley, N. Alamanos, and V. Lapoux, Phys. Rev. C 69 (2004) 064604.
- [22] S. Watanabe, Nucl. Phys. 8 (1958) 484.
- [23] A.J. Koning and J.P. Delaroche, Nucl. Phys. A713 (2003) 231.
- [24] R.V. Reid, Jr., Ann. Phys. (N.Y.) 50 (1968) 441.
- [25] V.I. Kukulín and R.S. Mackintosh, J. Phys. G: Nucl. Part. Phys. 30 (2004) R1.
- [26] S.G. Cooper, R.S. Mackintosh, and A.A. Ioannides, Nucl. Phys. A472 (1987) 101.